Modeling and Simulation of Metal-Semiconductor-Metal Photodetector using VHDL-AMS

Shu Wu and Sung-Mo Kang
Department of Electrical Engineering, University of California, Santa Cruz,
Santa Cruz, CA 95064, USA
wushu@soe.ucsc.edu

ABSTRACT

A circuit-level model of Metal-Semiconductor-Metal Photodetector (MSM-PD) was developed and implemented into VHDL-AMS simulator hAMster™. The model was derived for a one dimensional (1-D) structure from continuity equations. Both transient and steady-state simulations results match well with experimental data.

1. INTRODUCTION

Metal-semiconductor-metal photodetector has become popular in modern optical communication systems. It has several advantages over traditional p–i–n photodiodes [1]–[4]. Firstly, it has a planar structure, which is compatible with most semiconductor devices, making it ideal for optoelectronic integrated circuit (OEIC) applications. Secondly, because of its geometry, it has a lower capacitance for the same active area resulting in a lower (RC) time delay. Thirdly, the process for fabricating this device is very simple and is compatible with regular IC processes. With proper semiconductor material MSM-PD can work well with different transmission systems. For example, GaAs-based receivers [5] is suitable for short-wavelength short-distance communication links such as chip-to-chip optical interconnects, InGaAs-based receivers [6] can be used in long-distance optical communications in both 1.55 and 1.3 μm bands because of their small bandgaps, GaN-based photodetectors [7] in the wavelength range from 200 to 365 nm range are important components in a variety of military as well as commercial applications for their solar blinded, ultraviolet (UV) characteristic. Thus VHDL-AMS model for MSM-PD has become critical for system design and analysis.

2. MODELING AND SIMUALATION

The typical MSM-PD consists of interdigitaled metal fingers on top of the semiconductor layers, as shown in Figure 1. To reduce the dark current the Schottky barrier height can be adjusted by choosing proper material of the layer underneath the metal fingers. A buffer layer between the absorption layer and the substrate is needed to reduce the propagation of the defects in the substrate. The bias voltage is added to the metal fingers to create sufficient electrical field within the semiconductor layer. Light incident on the top surface of the photodector is absorbed to generate electron-hole pairs. The electrical field sweeps out the photogenerated carriers out of the device.

The 1-D cross section is shown in Figure 2. The 1-D assumption is valid if the photon absorption depth is much smaller than the distance between the adjacent metal fingers L, as shown in Figure 2. In fact, this condition is often satisfied in most practical situations, since absorption of photons deep in the substrate is typically avoided as it reduces the detector's responsivity and bandwidth [8].

The behavior of photo-generated carriers in MSM photodetector can be described by Poisson's equation and carrier continuity equations given below.

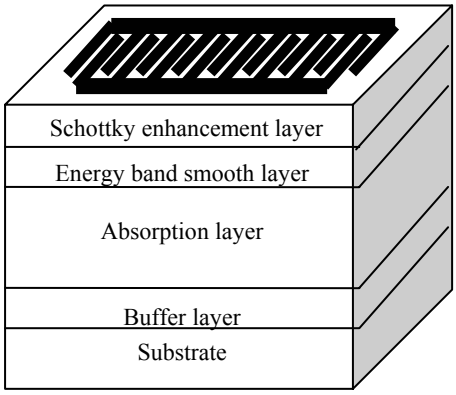

Fig. 1. Typical structure of a MSM-PD

Fig. 2. Cross section of interdigital area in MSM-PD

$$\varepsilon_0 \varepsilon_s \nabla^2 \psi = -q(p - n + N_D - N_A) \quad (1)$$

$$-\frac{1}{q}\nabla \bullet J_n - G + R_n + \frac{\partial n}{\partial t} = 0 \quad (2a)$$

$$\frac{1}{q}\nabla \bullet J_p - G + R_p + \frac{\partial p}{\partial t} = 0 \quad (2b)$$

where $R_{n/p}$ and G are the electron/hole recombination and generation rate, ψ is the electrostatic potential. J_n and J_p are electron and hole current density given by

$$J_n = q\mu_n nE + qD_n \nabla n \quad (3a)$$

$$J_p = q\mu_p pE - qD_p \nabla p \quad (3b)$$

Where $\mu_{n/p}$ and $D_{n/p}$ are the electron/hole mobility and diffusion constant, E is electric field. In order to get analytical solutions a uniform electric field is assumed and recombination rates are chosen to be n/τ_n and p/τ_p for electrons and holes respectively. $\tau_{n/p}$ is carrier lifetime.

2.1 Steady-state behavior

In steady-state, as the bias voltage raising the behavior of MSM photodetector can be treated for two cases. When the bias voltage is lower than the flat-band voltage, the potential barrier of the holes is lowered by the increased bias voltage, which results in rapid increase of the current. When the bias voltage reaches the flat-band voltage, the hole barrier approaches its limiting magnitude, the Schottky barrier height. Further increase in voltage will cause the current to increase slowly.

The photocurrent can be derived from above equations (1) to (3) and has the following form.

$$I_{ph} \propto I_0 \left(e^{\frac{qV}{nKT}} - 1 \right) \quad (4)$$

We also add tunneling current to the total current flowing out of the MSM-PD. The following equations show the total current in steady-state.

$$I_{dc} = I_0 \left(e^{\frac{qV}{nKT}} - 1 \right) + I_{ph0} \cdot A e^{-\frac{B}{V}}, V < V_{FB} \quad (5)$$

$$I_{dc} = I_{ph0} \cdot \left(1 + A e^{-\frac{B}{V}} \right), V \geq V_{FB} \quad (6)$$

where I_{dc} is the total current, V is the bias voltage, V_{FB} is the flat-band voltage, T is the temperature, K is the Boltzmann constant, and n, A, B, I_0 are fitting parameters. I_{ph0} is given below.

$$I_{ph0} = w(1-R)(1-e^{-\alpha d})\frac{\eta \cdot qp}{h\nu} \quad (7)$$

where w is area the ratio (area transparent to light/ area exposed to light), α is the absorption coefficient, d is the thickness of the absorption layer, η is the quantum efficiency, $h\nu$ is the photon energy, p is the incident light power.

We implement the model into hAMster™ using VHDL-AMS. The VHDL-AMS codes are shown in listing 1.

Listing 1. VHDL-AMS CODES OF MSM-PD DC MODEL

```
LIBRARY DISCIPLINES;
LIBRARY IEEE;
USE DISCIPLINES.ELECTROMAGNETIC_SYSTEM.ALL;
USE IEEE.MATH_REAL.ALL;
ENTITY MSMDC IS
  GENERIC (        T : REAL:=300.0;--k
                   d : REAL:=1.0e-4;--cm
           ...
           );
  PORT(TERMINAL p,m: ELECTRICAL;
                   quantity ph :real); --Interface ports.
END;
ARCHITECTURE behav OF MSMDC IS
  --quantity declarations.
  constant q :real:=1.6e-19;--C
  constant hc :real:=6.6262e-34;--Js
  constant k :real:=1.3807e-23;--J/k
  QUANTITY  Iph0 : REAL;
  QUANTITY  I0 : REAL;
  QUANTITY v_in ACROSS i_out THROUGH p TO m;
BEGIN
  ph==1.96e-6;--w
  Iph0==w*(1.0-R)*(1.0-exp(-1.0*alfa*d))*eta*q*ph/hc/miu;
  I0==Iph/(exp(q*Vfb**2/n/k/T)-1.0);
  if v_in<Vfb use
  i_out==I0*(exp(q*v_in*(2.0*Vfb-v_in)/(n*k*T))-1.0)+Iph*A*exp(-
1.0*B/v_in);
  else
  i_out==Iph*(1.0+A*exp(-1.0*B/v_in));
  end use;
END;
```

Table 1. Parameters in DC model for MSM-PD

Parameters (unit)	Value
T (K)	300
C0 (m/s)	3e8
λ (m)	1.31e-6
d (cm)	1e-4
w	1
η	0.5683
R	0.2
n	2.32
A (A)	0.534
B (V)	3.19

The simulation results shown in Fig. 3 have good agreement with Fig. 3 in [6]. The parameters used in simulation are listed in Table 1.

2.2 Temporal behavior

We can get temporal behavior for (1) to (3) by using variable separation and Fourier series technique. The electron distribution as a function of both position and time is

$$n(x,t) = \exp(-Ax)\sum_{k=1}^{\infty}\left\{T_{k,n}\cdot\exp(-\beta_{k,n}t)\cdot\sin(k\pi x/L)\right\}, \quad (8)$$

$$k = \{1,2,3...\}$$

where parameters A, β and $T_{k,n}$ are

$$A = \frac{\mu_n E}{2D_n} \quad (9)$$

$$\beta_{k,n} = \frac{\left(\frac{2D_n k\pi}{L}\right)^2 + {\mu_n}^2 E^2}{4D_n} + \frac{1}{\tau_n} \quad (10)$$

$$T_{k,n} = \frac{G_0 A}{L}\left[(-1)^{k+1}\exp(AL) - 1\right] \quad (11)$$

$$\cdot\left[\frac{1}{A^2 + (k-1)^2\pi^2/L^2} - \frac{1}{A^2 + (k+1)^2\pi^2/L^2}\right]$$

The hole distribution has the same form with electron except using $-\mu_p$, D_p and τ_p instead of μ_n, D_n and τ_n corresponding to hole quantities. The pulse response shown below can be obtained by putting (8) back to (1) to (3). The parameters in (12) and (13) have same meanings as before.

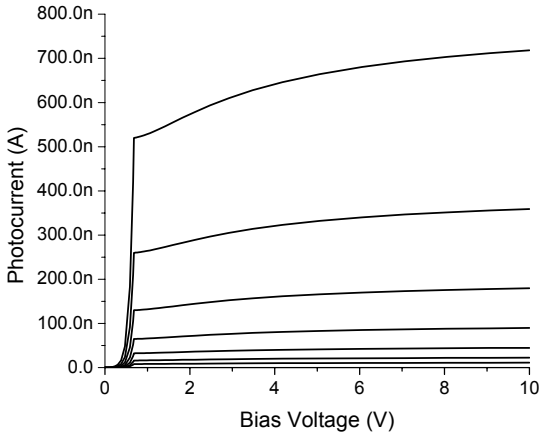

Fig. 3. DC response of MSM-PD. (light intensity attenuated at 3 dB steps from 1.96 μw with a 1.31 μm laser)

$$J_{n\_pulse}(t) = qD_n\sum_{k=1}^{\infty}\left[T_{k,n}\cdot\frac{k\pi}{L}\cdot\exp(-\beta_{k,n}t)\right] \quad (12)$$

$$J_{p\_pulse}(t) = -qD_p\cdot\exp(-AL)\cdot\sum_{k=1}^{\infty}\left[T_{k,p}\cdot\frac{k\pi}{L}\cdot(-1)^k\exp(-\beta_{k,p}t)\right] \quad (13)$$

To reduce the complexity we can use the following equation to model the pulse response of MSM-PD.

$$J_{pulse} = J_{pulse0}\cdot\sum_{n=1}^{\infty}\frac{2}{n\pi}\sin\left(\frac{n\pi}{2}\right)g_n(t-t_0) \quad (14)$$

$$g_n(t) = \lambda_n^2\cdot e^{-\lambda_n^2 t},\ \lambda_n^2 = \frac{(n\pi)^2}{\tau}$$

where J_{pulse0} is fitting parameter, τ is transit time.

Simulation was done by using (13) corresponding to the experiment data in references [9] and [10]. Fig. 4 is corresponds to Fig 4 in [9] and Fig. 5 is corresponds to Fig 1 in [10]. The parameters used for simulation are shown in the figures. Our simulation results matched those in [9], [10].

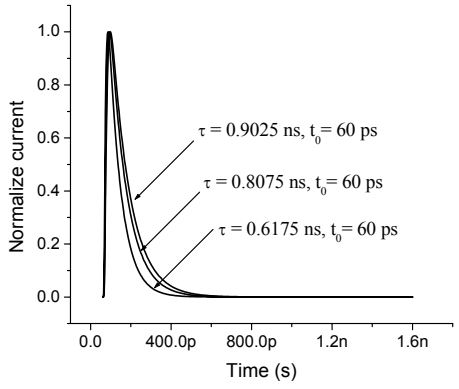

Fig. 4 Simulation results of pulse response of MSM-PD in [9]

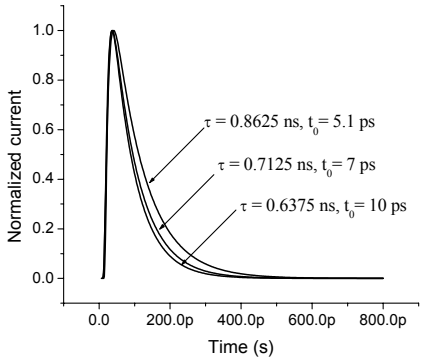

Fig. 5 Simulation results of pulse response of MSM-PD in [10]

The frequency response of MSM-PD can be obtained by taking Fourier transform of (12) and (13), resulting in

$$J_n(\omega) = qD_n \sum_{k=1}^{\infty} \left[T_{k,n} \cdot \frac{k\pi}{L} \cdot \frac{1}{\beta_{k,n} - i\omega} \right] \tag{14}$$

for electrons and holes,

$$J_p(\omega) = -qD_p \cdot \exp(-AL) \cdot \sum_{k=1}^{\infty} \left[T_{k,p} \cdot \frac{k\pi}{L} \cdot (-1)^k \frac{1}{\beta_{k,p} - i\omega} \right] \tag{15}$$

The 3-dB frequency for the electrons is $f_{-3dBn} = \beta_{k,n}/2\pi$ and for holes is $f_{-3dBp} = \beta_{k,p}/2\pi$. We did frequency response simulation with 0.8 V bias voltage using (14) and (15). The plots are shown in Fig 6. Simulation results show that the hole is the main limitation of the whole photodetector bandwidth due to its slow mobility.

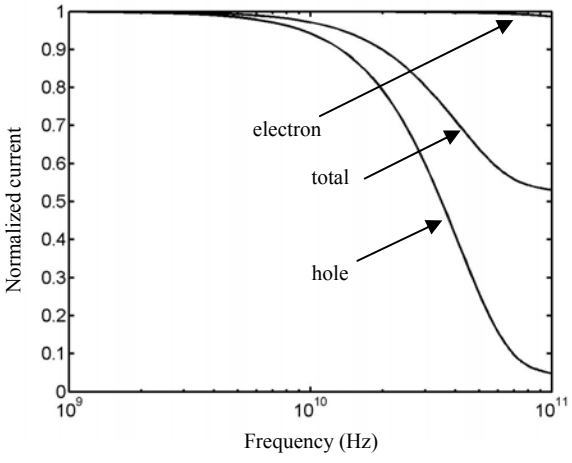

Fig. 6 Frequency response of electron, hole and total current in an MSM-PD

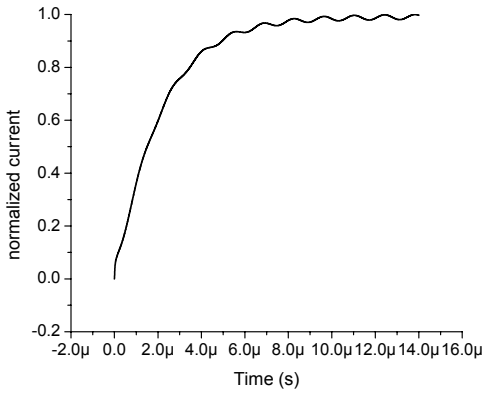

Fig 7. Simulation result of the MSM-PD response under sine function input

Other input response of the photodetector can be obtained by taking the convolution of the pulse response shown in (16) and (17) with the input function as

$$J_{n,p}(t) = J_{pulse}(t) * S(t) = \int_0^t J_{n.p\_pulse}(t - t_0) \cdot S(t_0) dt_0 \tag{16}$$

where S(t) is the incident light waveform function and J_{pulse} is the pulse response shown in (14). To demonstrate this feature we simulate the MSM-PD response under sinusoidal optical input. The simulation result is shown in Fig. 7. The transit time was chosen to be 19.6 μs in simulation.

3. SUMMARY

A circuit-level model of MSM-PD was demonstrated in this paper. The model has been implemented into VHDL-AMS simulator hAMster^{TM} including steady-state, temporal and frequency domain behavior of MSM-PD. The model was derived in a one dimensional (1-D) structure from continuity equations. Both time-dependent and steady-state simulations have good agreements with published experimental data.

4. REFERENCES

[1] Berger P R, "MSM photodiode" *IEEE Potentials,* 1996, pp1525–9

[2] Soole J B D and Schumacher H, "InGaAs metal–semiconductor–metal photodetectors for long wavelength optical communications", *IEEE J. Quantum Electron.* Vol. 27, 1991, pp 737–52

[3] P. Fay, W. Wohlmuth, A. Mahajan, C. Caneau, S. Chandrasekhar and I. Adesida, "A comparative study of integrated photoreceivers using MSM/HEMT and PIN/HEMT technologies", *IEEE Photon. Technol. Lett.,* vol.10, 1998, pp582–4

[4] Martin E A, Vaccaro K, Spaziani S M and Lorenzo J P, "Backside illumination processing technology for InGaAs/InAlAs/InP photofets and MSMs", *Microelectron.J.* , vol. 26, 1995, pp 497–505

[5] S D Lin and C P Lee, "GaAs metal–semiconductor–metal photodetectors with low dark current and high responsivity at 850 nm", *Semicond. Sci. Technol*. , vol. 17, pp. 1261–1266, 2002

[6] A. Xiang, W. Wohlmuth, P. Fay, S. M. Kang and I. Adesida, "Modeling of InGaAs MSM photodetector for Circuit-Level Simulation", *J. Lightwave Technol.,* vol. 14, No. 5, pp 716, 1996

[7] S. Wang, T. Li, J. M. Reifsnider, B. Yang, C. Collins, A. L. Holmes, Jr. and J. C. Campbell, "Schottky Metal-Semiconductor-Metal Photodetectors on GaN Films Grown on Sapphire by Molecular Beam Epitaxy", *IEEE J. Quantum Electron,* vol. 36, No. 11, pp1262, 2000

[8] Anthony W. Sarto and Bart J. Van Zeghbroeck, "Photocurrents in a Metal–Semiconductor–Metal Photodetector", *IEEE J. Quantum Electron.,* vol. 33, No. 12, pp 2188, 1997

[9] V. Krishnamurthy, M. C. Hargis, and M.R. Melloch, " A 4-GHz Large-Area (160000 μm^2) MSM-PD on ITG-GaAs", *IEEE photonics technology letters*, vol. 12, No. 1, pp. 71, 2000

[10] K. Aliberti, M. Wraback, M. Stead, P. Newman, and H. Shen, " Mesurements of InGaAs metal-semiconductor-metal photodetectors under high-illumination conditions", *Applied Physics letters*, vol. 80, No. 16, pp. 2848, 2002

[11] Ito M and Wada O, "Low dark current GaAs metal–semiconductor–metal (MSM) photodiodes using WSi_x contacts", *IEEE J. Quantum Electron.,* vol. 22, pp 1073–7, 1986

[12] Chan P T, Choy H S, Shu C and Hsu C C, "High-performance InP/Ga0.47In0.53As/InP metal–semiconductor–metal photodetectors with a strained $Al_{0.1}In_{0.9}P$ barrier enhancement layer", *Appl. Phys. Lett.,* vol. 67, pp. 1715–7, 1995

[13] W. Wohlmuth, M. Arafa, A. Mahajan, P. Fay and I. Adesida, "InGaAs metal–semiconductor–metal photodetectors with engineered Schottky barrier heights", *Appl. Phys.Lett.,* vol. 69, pp. 3578–80, 1996

[14] E. Sano, "A Device Model for Metal-Semiconductor-Metal Photodetectors and its Applications to Optoelectronic Integrated Circuit Simulation", *IEEE Trans. On Electron Devices,* vol. 37, No.9, pp 1964, 1990

[15] Sze S M, Coleman D J, Loya J R and Loya A "Current transport in metal–semiconductor–metal (MSM) structures", *Solid-State Electron.,* vol. 14, pp.1209–18, 1971

[16] Sze S M, *Physics of Semiconductor Devices* 2nd edition, (New York: Wiley), 1981